

2-D soil zymography: accounting for the spatial variation of pH

Andrey Guber* and Alexandra Kravchenko

Department of Plant, Soil and Microbial Sciences, Michigan State University, East Lansing, MI.

Corresponding author: akguber@msu.edu

ABSTRACT

Soil zymography is commonly used to quantify spatial distribution of hydrolytic enzyme activities on soil and plant root surfaces. It is recommended to adjust pH in zymography substrates and calibration solutions with respect to soil/root pH. However, pH values may vary greatly within a few mm of plant rhizosphere, potentially altering the distribution of pH in zymography membranes. Despite the fact that the effect of pH on the calibration of zymography membranes is generally known, its potential impact on zymography results is unaccounted for in processing zymography images and calculations of enzyme activity. In this study we assessed the effect of pH variations on the persistency of the methylumbelliferone (MUF) calibration. The studied pH values ranged from 4.5 to 7.5. The MUF calibration curves greatly deviated from that at a reference pH of 6.5, with a marked nonlinear increase of deviation with greater membrane brightness. We suggest that the problem can be partially alleviated by reducing the membrane incubation time. However, such deviations suggest the need for a more comprehensive resolution via mapping pH and using pH-specific calibrations to process zymography images. We developed a MATLAB code to implement a pixel-based correction of enzyme activity for pH in processing time-lapse zymography images.

Keywords: Soil hydrolytic enzymes, *in situ* membrane zymography, MUF calibration, pH

Abbreviations: methylumbelliferone, MUF; greyscale value, G-value; time-lapse zymography, TLZ.

Soil 2-D membrane zymography is commonly used to map and quantify spatial distributions of hydrolytic enzyme activities on soil and plant root surfaces. The method consists of incubating a membrane saturated with an enzyme-specific fluorogenic substrate on the surface of soil/root samples. To produce a map of enzyme activity either the incubation is accompanied by recording a sequence of membrane images (e.g., from 30 to 45 photographs at one minute interval)

generated by a fluorescent product: methylumbelliferone (MUF) (i.e. time-lapse zymography (TLZ) developed by Guber et al., 2021) or a single image of the membrane is taken at the end of the incubation (i.e. traditional zymography developed by Spohn & Kuzyakov, 2014; Sanaullah et al., 2016) in ultraviolet light. Then zymography images are converted to MUF contents using a single calibration curve obtained using standard MUF solutions. Since enzyme activity changes with pH (Tabatabai, 1994; Turner, 2010), it is recommended to select a buffer for the substrate and MUF calibration solutions with pH similar to that in the studied soil (Niemi and Vepsäläinen, 2005; German. et al., 2011; Turner, 2010; Burns et al., 2013; Razavi et al., 2017; Razavi, et al. 2019; Bilyera and Kuzyakov, 2024). Note, that chitinase (4-MUF-N-acetyl- β -D-glucosaminide) and phosphatase (4-MUF phosphate) are exceptions, in which the substrates spontaneously dissociate from MUF at pH < 5.0 and pH > 6.5. Unfortunately, using pH similar to that in the studied soil is not always achievable in the studies of soil rhizosphere, where pH values between root and soil surfaces may differ by several units (Rudolph et al., 2013; Ma et al., 2019). Direct measurements showed that the volume of substrate solution within a zymography membrane, which is just 0.1 mm thick, is relatively small (i.e. $7.4 \pm 1.3 \mu\text{l cm}^{-2}$) as compared with the water content of soil/roots in the ~ 0.2 mm thick soil layer under the membrane that is being surveyed during zymography (i.e., 80-160 $\mu\text{l cm}^{-2}$). The result of enzyme transport experiments in undisturbed sand, sandy loam and loam soil columns demonstrated that pH in soil remained mostly unchanged after 2-3 pore volumes of solution have been replaced by an applied solutions with higher pH values (Guber et al., 2022). Therefore, a relatively small volume and a slow diffusion of the substrate moving from the membrane to the soil/root surface during zymography is unlikely sufficient to considerably alter the pH values in the underlying soil layer, and its effect on enzyme reactions can be regarded as negligible. At the same time, since zymography membranes do not change chemical composition of the solution, it is reasonable to suggest that the volume of the solution in soil pores and MUF diffusing from the underlying soil layer back to the membrane and replacing the substrate in it can be considerable. Therefore, the pH in diffusion influx may markedly change the pH in the small volume of the membrane solution in contact with soil/root surfaces. It has been shown (Niemi and Vepsäläinen, 2005), that even a minor alteration of pH in the membrane can result in substantial changes of MUF brightness detected by the camera in the enzyme active zones. The authors observed an eight-time increase in MUF brightness with increasing pH levels from 4.5 to 7.5 units, and a five-time

increase for pH changes from 6 to 7.5 units, respectively. Their observations suggest that using a calibration curve built at a single pH-level can result in potentially erroneous estimates of enzyme activities in the portions of the studied soil/root surfaces where pH deviates from that in the substrate solution. The effect of pH on MUF brightness in soil studies has been reported by Disk (2011) and Giles et al, (2018) and attributed to changes of MUF protonation state and its brightness with pH changes from acid to alkaline conditions (Zhi et al., 2013). Giles et al, (2018) assumed that peak of MUF fluorescence is affected by methanol used to prepare the calibration solutions and suggested to use either calibration filters with excess of MUF incubated with solutions of known enzyme activity, or calibration filters soaked in a range of MUF concentrations and incubated in excesses of enzyme activity. While both approaches are meaningful, to our best knowledge, they have not been experimentally validated yet.

As an alternative, we suggest accounting for changes of MUF calibration curve with pH when processing zymography images. Our goals were: (1) to quantify the effect of the pH on MUF calibration in zymography membranes; and (2) to suggest an approach to account for the variation of pH values in zymography calculations.

Calibration testing experiment setup: The MUF standard solutions of 0.0625, 0.125, 0.25, 0.5, 1.0, 2.5, 5.0 and 10.0 mM were prepared using 0.1 M MES buffer (M3671, Sigma-Aldrich, Inc., St. Louis, MO, USA) with pH=3.5 and adjusted to pH values of 4.5, 5.0, 5.5, 6.0, 6.5, 7.0, and 7.5 using NaOH (1 M). The standards were kept for 30 min to stabilize their fluorescence (Razavi et al., 2019; Burns et al., 2013). A 10 μ l drop of each standard solution was applied on the surface of a 1 x 1 cm hydrophilic polyamide membrane (100- μ m thick, Tao Yuan, China). A total of 168 MUF calibration membranes were used (8 MUF concentrations x 7 pH levels x 3 replicates). The membranes were grouped according to the pH levels and replications (8 membranes in each group). Then the images were taken under UV light immediately after MUF application using a Canon EOS Rebel T6 camera with a Canon EF 75–300 mm f/4–5.6 III Telephoto Zoom Lens (Canon U.S.A., Inc.) connected to a computer and controlled by Helicon remote software (Helicon Soft Ltd., Ukraine). The size of the pixels on the calibration images was 17 μ m. We used a 20W circline blacklight blue fluorescent bulb (FC8T9/BLB, Bulborama, Las Vegas, NV USA) with diameter of 20 cm as a source of UV.

The calibration images (Fig. 1) revealed that brightness increased with as pH in the calibration solutions increased from 4.5 to 7.5. Visually, the increase was more pronounced in membranes with higher MUF contents.

Image processing: The “blue (B)” channel was extracted from the RGB images and used for the calibration. This approach differs from the standard 8-bit transformation of the RGB images commonly used in 2D zymography. In fact, it is more consistent with the bench scale and microplate enzyme assays with emission wavelength 415 - 460 nm (Deng et al., 2013) and generates lower random noise, broader histogram, and higher peak greyscale values (G-values) as compared with the “red (R)”, “green (G)” channels and RGB images converted to 8-bit format. We built on the MUF calibration approach developed by Guber et al. (2019) with a minor modification. Specifically, for each MUF calibration membrane we subtracted the background, which was estimated as an average G-value within MUF-free area of the membrane. Then, the calibration equation was applied to each pixel i of every membrane j in a form:

$$MUF_i^j = b \cdot \exp(c \cdot G_i^j) - a \quad (1)$$

where MUF_i^j is MUF content in i -pixel of the calibration membrane j , [nmol mm⁻²]; G_i^j is the G-value in the same pixel after background subtraction, [-]; a , b , and c are empirical parameters with units: [nmol mm⁻²], [nmol mm⁻²], and [-], respectively. A MATLAB code was developed that implemented the Levenberg–Marquardt method (Marquardt, 1963) to fit the calibration parameters a , b , and c in Eq.(1) to the MUF mass in each calibration membrane. The weight factors were introduced to the objective function Z as reciprocal values of MUF mass to eliminate the effect of large MUF values on the fitting parameters:

$$Z = \min \sum_j (1 - \sum_i^j (MUF_i^j) / MUF_{appl}^j)^2, 1 \leq j \leq 168 \quad (2)$$

where MUF_{appl}^j are applied mass of MUF in each calibration membrane j [nmol].

Calibration parameters: The goodness of fit metrics for Eq.(1) were $R^2 = 0.94 \pm 0.08$ (mean \pm one standard deviation) and $MRE = 7.9 \pm 3.1\%$ (mean relative error of MUF_{appl}^j), indicating acceptable accuracy of the fitted calibration function. The parameters a and b did not demonstrate a clear trend with pH. The parameter a was numerically large for pH=4.5 and pH=5.5 as compared with the other pH levels (Fig. 2a). The parameter b was of the same order of magnitude in the pH range 4.5 to 6.5, then decreased abruptly at pH=7.0 and 7.5 (Fig. 2b). A

clear decrease with increasing pH was observed for parameter c (Fig. 2c). At constant values of parameter b , parameter c controls the slope of the MUF calibration curve (Eq.(1)), which is:

$$\frac{\partial MUF_i^j}{\partial G_i^j} = b \cdot c \cdot \exp(c \cdot G_i^j) \quad (3)$$

The larger c values, the faster MUF content increases with G_i^j . The trend in Fig. 2c was consistent with visual analysis of the calibration images. For the same MUF contents, the brightness of the images increased with the pH level.

Calibration curves: A vast majority of zymography studies lacks information on pH values in substrates and calibration solutions. Therefore, in this study we used MUF calibration measured at pH=6.5 as a reference curve since this pH value has been used in original publication of this method (Sanaullah et al., 2016). The shape of the pH=6.5 calibration curve was strongly non-linear (Fig. 2d dashed line). Also reported on Fig. 2d are deviations of the MUF calibration curves from that measured at pH=6.5, i.e., $\Delta MUF_{pH} = MUF_{pH} - MUF_{6.5}$. The decreasing trend in parameter c with increasing pH translated into progressive changes in such deviations. The ΔMUF_{pH} values increased non-linearly with the image brightness, indicated by G-values, and were most pronounced starting from G-values = 35-50 (Fig. 2d, solid lines). The non-linear trend in ΔMUF_{pH} was associated with non-linearity of the MUF calibration curves in G-values >35. Notably, larger ΔMUF_{pH} corresponded to larger deviation of pH in the standard solutions from 6.5 and were positive for pH < 6.5. The observed trends implied that using a single calibration curve for pH=6.5 to calculate enzyme activity may considerably underestimate MUF contents, and thus enzyme activity, in the locations with pH lower than 6.5 (e.g., root tips), while overestimating it in the locations with pH > 6.5.

Experiments and modeling (Guber et al., 2018, 2021) have shown that longer incubation time, in general, results in large MUF production, its greater diffusion to the membrane, and thus brighter images (i.e. higher G-values). Therefore, one way to moderate the effect of pH on calculations of enzyme activity could be via reducing brightness of zymography images by shortening incubation time. However, this is not always possible, particularly for traditional single snapshot zymography in the rhizosphere, where brightness between soil matrix and roots may differ substantially (as follows from Fig. 1- Fig-3, Ma et al., 2019) in G-values, so 1-2 hour and longer incubation times are frequently used to detect low activity in soil (Spohn et al., 2013; Sanaullah et al., 2016; Razavi et al., 2016). The effect of pH became pronounced for our settings

starting from relatively low G-values (i.e. 30-50), which were derived from blue channel of the RGB image. This range roughly corresponds to G-values of 20-25 for 8-bit images, obtained by direct conversion of RGB images without splitting channels, and is typically observed in zymograms of β -glucosidase and phosphatase in enzyme active areas on soil/root surfaces. Therefore, shortening zymography time may not be always achievable for the traditional zymography. Contrary to the traditional zymography, TLZ does not require shorter time, because zymography images are taken at one minute interval during 30-45 minute incubation. Therefore, an optimal range of G-values can be defined in each individual pixel of zymogram from time series of G-values obtained from zymography sequences in these pixels.

As an alternative, TLZ can be combined with pH mapping (Ma et al., 2019) that enables correcting MUF values using pH specific calibrations. The correction has been implemented within the MATLAB procedure currently used for TLZ image processing. The code first transforms the calibration curves measured at different pH values into lookup tables with integer G-values varied from 1 to 255 and pH varied from 4.5 to 7.5 at increment 0.1. The size of the lookup table is 255 x 31 (G-values x pH), that enabled fast calculations of MUF based on pH and G-values at any time moment in individual pixels of zymograms. Then the code calculates the activity in each individual pixel of membrane, based on time series of MUF content in these pixels with correction for MUF losses due to its omnidirectional diffusion in soil.

Conclusions and implementation: This study demonstrated potential effects of pH on results of 2D membrane zymography originated from changing MUF brightness with pH values. The problem can be remediated by shortening the duration of membrane incubation to reduce the brightness of zymography images below the values at which the pH effect becomes pronounced or by combining membrane zymography with pH mapping and MUF calibration for multiple pH levels. The G-scale range can be specific for light and camera settings and includes G-values corrected for the background autofluorescence and quenching. Here we used pH=6.5 as a reference point to demonstrate the effect of pH on MUF calibration potential impact on results of activity calculation. But for the traditional (single snapshot) zymography, the reference point can be adjusted to pH level in soil or roots with respect to the research objectives, when calibration is performed for expectable range of the pH values. For the TLZ, the pH image is processed jointly with zymograms, and MUF values are corrected for pH in individual pixels of zymograms using the look-up table generated from the calibration curves at different pH levels. Combining

zymography with pH mapping is potentially beneficial for interpretation of the spatial variability of enzyme activity caused by the spatial variability of pH and by deviations in the pH values from those optimal for enzyme reactions.

Declaration of competing interest

The authors declare that they have no known competing financial interests or personal relationships that could have appeared to influence the work reported in this paper.

Data availability

Data and MATLAB code are available from the first author upon request.

Acknowledgments

Support for this research was provided by the Great Lakes Bioenergy Research Center, U.S. Department of Energy, Office of Science, Office of Biological and Environmental Research (Award DE-SC0018409), by the National Science Foundation Long-term Ecological Research Program (DEB 2224712) at the Kellogg Biological Station, and by USDA-NIFA, Award no. 2022-67019-36104.

REFERENCES

- Bilyera, N., Kuzyakov, Y., 2024. Soil zymography: A decade of rapid development in microbial hotspot imaging. *Soil Biology and Biochemistry*, v. 189, <https://doi.org/10.1016/j.soilbio.2023.109264>
- Burns, R. G., DeForest, J. L., Marxsen, J., Sinsabaugh, R. L., Stromberger, M. E., Wallenstein, M. D., Weintraub, M.N., Zoppini, A., 2013. Soil enzymes in a changing environment: Current knowledge and future directions. *Soil Biology and Biochemistry*, 58(December 2018), 216–234. <https://doi.org/10.1016/j.soilbio.2012.11.009>
- Deng, S., Popova, I. E., Dick, L., & Dick, R., 2013. Bench scale and microplate format assay of soil enzyme activities using spectroscopic and fluorometric approaches. *Applied Soil Ecology*, 64, 84–90. <https://doi.org/10.1016/j.apsoil.2012.11.002>

- Dick, R.P., 2011. *Methods of Soil Enzymology*. Soil Science Society of America, Madison, Wisconsin, USA.
- German, D. P., Weintraub, M. N., Grandy, A. S., Lauber, C. L., Rinkes, Z. L., & Allison, S. D., 2011. Optimization of hydrolytic and oxidative enzyme methods for ecosystem studies. *Soil Biology and Biochemistry*, 43(7), 1387–1397.
<https://doi.org/10.1016/j.soilbio.2011.03.017>
- Giles, C. D., Dupuy, L., Boitt, G., Brown, L. K., Condrón, L. M., Darch, T., Blackwell, M.S.A. , Menezes-Blackburn, D., Shand, C.A., Stutter, M.I., Lumsdon, D.G., Wendler, R. , Cooper, P., Wearing, C., Zhang, H., Haygarth, P.M., George, T. S., 2018. Root development impacts on the distribution of phosphatase activity: Improvements in quantification using soil zymography. *Soil Biology and Biochemistry*, 116, 158–166.
<https://doi.org/10.1016/j.soilbio.2017.08.011>
- Guber, A., Kravchenko, A., Razavi, B. S., Uteau, D., Peth, S., Blagodatskaya, E., & Kuzyakov, Y., 2018. Quantitative soil zymography: Mechanisms, processes of substrate and enzyme diffusion in porous media. *Soil Biology and Biochemistry*, 127(September), 156–167.
<https://doi.org/10.1016/j.soilbio.2018.09.030>
- Guber, A. K., Kravchenko, A. N., Razavi, B. S., Blagodatskaya, E., & Kuzyakov, Y., 2019. Calibration of 2-D soil zymography for correct analysis of enzyme distribution. *European Journal of Soil Science*, 70(4), 715–726. <https://doi.org/10.1111/ejss.12744>
- Guber, A., Blagodatskaya, E., Juyal, A., Razavi, B. S., Kuzyakov, Y., & Kravchenko, A., 2021. Time-lapse approach to correct deficiencies of 2D soil zymography. *Soil Biology and Biochemistry*, 157(November 2020), 108225.
<https://doi.org/10.1016/j.soilbio.2021.108225>
- Ma, X., Mason-Jones, K., Liu, Y., Blagodatskaya, E., Kuzyakov, Y., Guber, A., Dippold, M.A., Razavi, B. S., 2019. Coupling zymography with pH mapping reveals a shift in lupine phosphorus acquisition strategy driven by cluster roots. *Soil Biology and Biochemistry*, 135(May), 420–428. <https://doi.org/10.1016/j.soilbio.2019.06.001>
- Marquardt, D. W., 1963. An algorithm for least-squares estimation of nonlinear parameters. *Journal of the Society for Industrial & Applied Mathematics*, 11, 431–441.

- Niemi, R.M., and Vepsäläinen, M., 2005. Stability of the fluorogenic enzyme substrates and pH optima of enzyme activities in different Finnish soils. *Journal of Microbiological Methods* 60, 195-205.
- Razavi, B.S., Zarebanadkouki, M., Blagodatskaya, E., Kuzyakov, Y., 2016. Rhizosphere shape of lentil and maize: spatial distribution of enzyme activities. *Environmental Modelling and Software* 79, 229–237. <https://doi.org/10.1016/j.soilbio.2016.02.020>.
- Razavi, B. S., Hoang, D., & Kuzyakov, Y., 2017. Visualization of enzyme activities in earthworm biopores by in situ soil zymography. *Methods in Molecular Biology*, 1626, 229–238. https://doi.org/10.1007/978-1-4939-7111-4_22
- Razavi, B. S., Zhang, X., Bilyera, N., Guber, A., & Zarebanadkouki, M., 2019. Soil zymography: Simple and reliable? Review of current knowledge and optimization of the method. *Rhizosphere*, 11(March), 100161. <https://doi.org/10.1016/j.rhisph.2019.100161>
- Rudolph, N., Voss, S., Moradi, A. B., Nagl, S., Oswald, S. E., 2013. Spatio-temporal mapping of local soil pH changes induced by roots of lupin and soft-rush. *Plant and Soil*, 369(1–2), 669–680. <https://doi.org/10.1007/s11104-013-1775-0>
- Sanaullah, M., Razavi, B. S., Blagodatskaya, E., & Kuzyakov, Y., 2016. Spatial distribution and catalytic mechanisms of β -glucosidase activity at the root-soil interface. *Biology and Fertility of Soils*, 52(4), 505–514. <https://doi.org/10.1007/s00374-016-1094-8>
- Spohn, M., Carminati, A., Kuzyakov, Y., 2013. Soil zymography - a novel in situ method for mapping distribution of enzyme activity in soil. *Soil Biology and Biochemistry* 58, 275–280. <https://doi.org/10.1016/j.soilbio.2012.12.004>.
- Spohn, M., Kuzyakov, Y., 2014. Spatial and temporal dynamics of hotspots of enzyme activity in soil as affected by living and dead roots—a soil zymography analysis. *Plant and Soil* 379, 67–77.
- Zhi, H., Wang, J., Wang, S., Wei, Y., 2013. Fluorescent properties of hymecromone and fluorimetric analysis of hymecromone in compound dantong capsule. *Journal of Spectroscopy* 2013, 9.

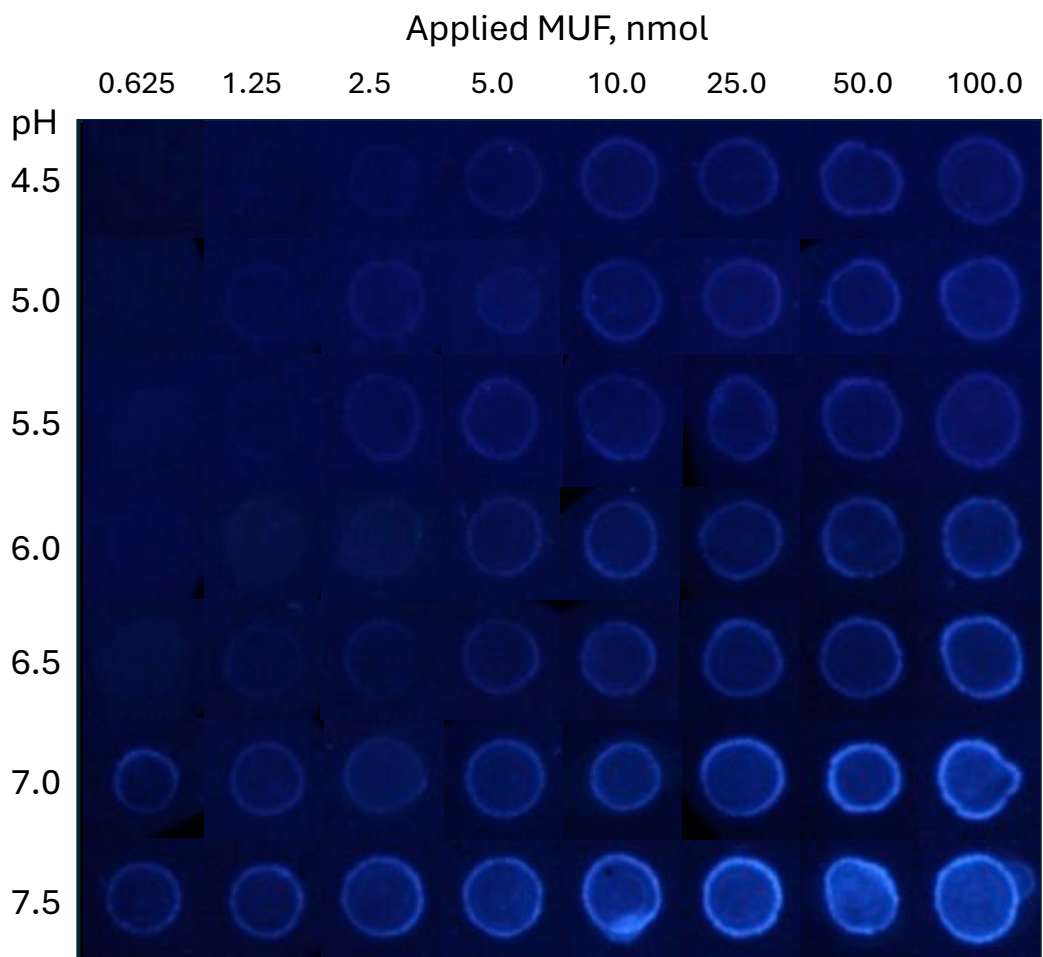


Fig. 1. Original images of the calibration membranes taken at different pH levels before correction for the background brightness.

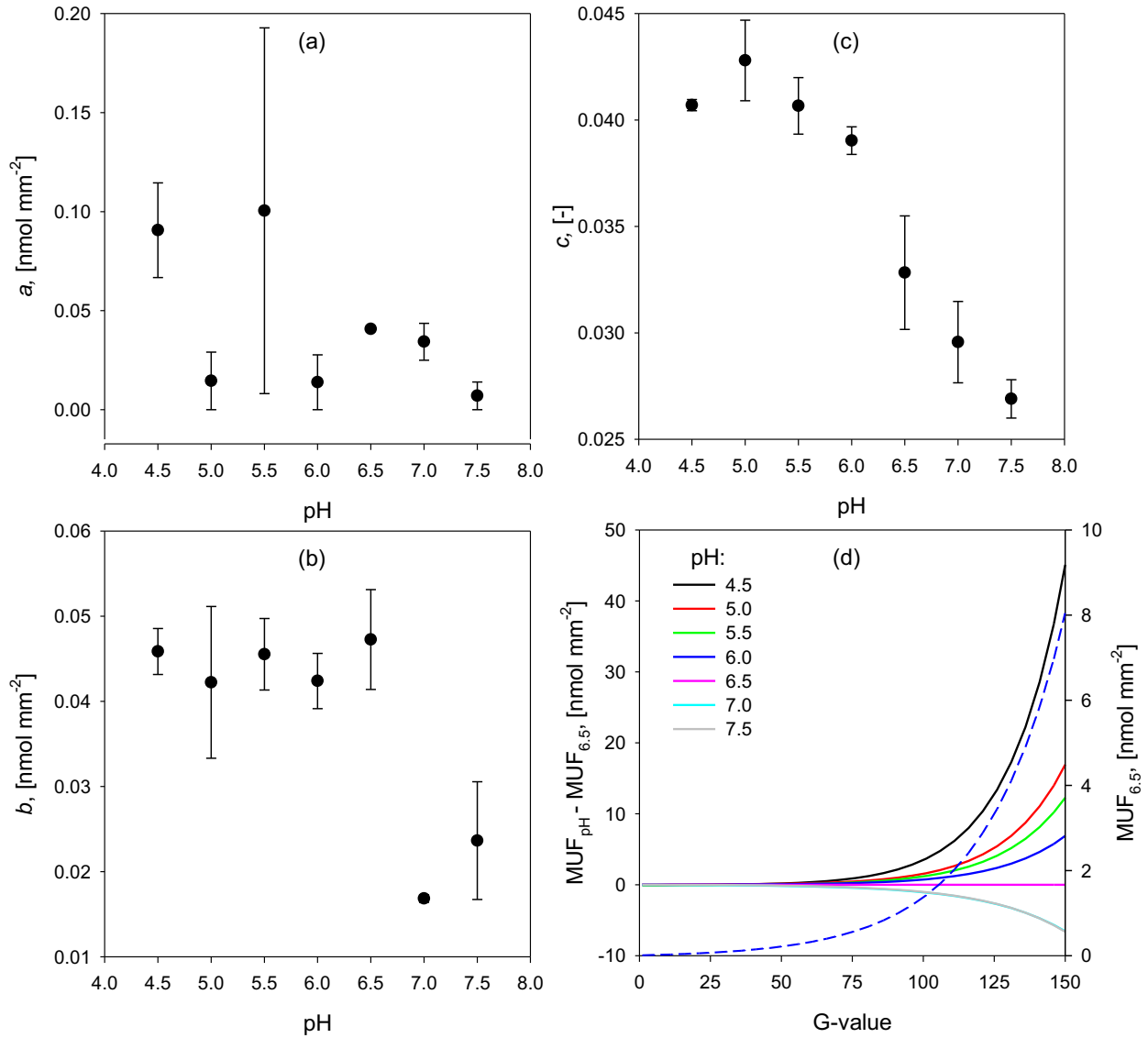


Fig. 2. Calibration parameters for Eq.(1): $MUF_i^j = b \cdot \exp(c \cdot G_i^j) - a$ at seven pH levels (a-c). Error bars represent standard errors (n=3). $MUF_{6.5}$ calibration curve measured for pH=6.5 ((d) blue dashed line, right Y axis), and deviation of the calibration curves measured at six pH levels from that for $MUF_{6.5}$ (d) solid lines, left Y axis pH). Each line represents an average among three replicated calibrations obtained for the same pH level. Line for pH=7.0 overlaps with that for pH=7.5.